Linear muffin-tin orbital calculation of local electronic and magnetic properties in $(Fe_{1-x}Ni_x)_4N$ $(0 \leq x \leq 1.0)$

Yong Kong* and Fashen Li
Department of Physics, Lanzhou University, Lanzhou 730000, China
(Received 21 January 1997; revised manuscript received 23 May 1997)

The spin-polarized linear muffin-tin orbital method has been applied to calculate the electronic structure of $(Fe_{1-x}Ni_x)_4N$ $(0 \leq x \leq 1.0)$. It is of interest that the band structure and the electronic and magnetic properties of $(Fe_{1-x}Ni_x)_4N$ depend sensitively on the substitution of Ni for Fe. The investigation of the dependences of the local electronic and magnetic properties on the Ni content indicates a change of interaction between atoms with increasing x. The calculated results reveal a discrepancy between the changes of the local magnetic moment and the hyperfine field of Fe and Ni at both sites due to the transferred hyperfine field. The volume effect of the substituted Ni has been distinguished from its chemical-bonding effect. The dependence of the conduction-electron polarization of the nuclei on interatomic distance indicates a Ruderman-Kittel-Kasuya-Yosida–like character of interatomic interaction. Some numerical results are given and the calculated results agree qualitatively with the experimental results. [S0163-1829(98)01202-8]

I. INTRODUCTION

In recent years great attention has been given to iron nitrides. Among these, γ'-Fe_4N (Ref. 1) has long been the object of extensive experimental[2–5] and theoretical[6–9] studies and considered as a potential candidate for high density recording materials due to excellent magnetic properties in combination with a better chemical stability. To improve the magnetic properties and the chemical stability of γ'-Fe_4N, one has synthesized and studied $(Fe,TM)_4N$ (Refs. 10–12) by the substitution of a second transition metal (TM) (TM =Ni,Sn,Mn, and so on) for iron. It has been found that the chemical stability and the mechanical ductility of the γ'-Fe_4N compound can be improved by the substitution of Ni.[13,14] The investigation of thermal expansion and force magnetostriction of Fe_3NiN showed similarities with the Fe-Ni Invar alloys.[15,16] It is of interest to prepare and study the $(Fe,Ni)_4N$ compounds with higher Ni content. Previous works[17,18] have reported $(Fe,Ni)_4N$ with a Ni concentration up to 60 at. %. The results indicated that the substitution of Ni for Fe decreases the lattice constants of systems and reduces the average hyperfine field $(\overline{H_{hf}})$. In comparison with the $Fe_{1-x}Ni_x$ alloy, the lattice-spacing expansion $\delta a/a$ is 5.3% after nitrogenization. It is attractive to study the substitutional and interstitial effects of Ni and N atoms, systems that merit further investigation. Recently single phase powder of $FeNi_3N$ has been successfully prepared[19] and Williamson *et al.*[20] have reported the $FeNi_3N$ phase by N^+ ion implantation. To our knowledge, theoretical results on $(Fe_{1-x}Ni_x)_4N$ with high Ni content have hardly been reported except for the work on Fe_3NiN by Mohn *et al.*,[15] which is assumed to be a completely ordered compound.

In order to investigate the local electronic and magnetic structure of $(Fe_{1-x}Ni_x)_4N$ in this paper, the self-consistent spin-polarized linear muffin-tin orbital (LMTO) method has been employed to calculate the electronic structure of $(Fe_{1-x}Ni_x)_4N$ with various Ni content. According to our theoretical results, the local electronic and magnetic properties of the system and the substituted effects of the Ni atoms are discussed in detail and some numerical results are presented.

According to the results of x-ray diffraction,[17] $(Fe_{1-x}Ni_x)_4N$ crystallizes in a Perovskite-type structure[21] such as γ'-Fe_4N with two inequivalent Fe crystalline sites, which are the corner site (marked c) and the face-centered site (marked f). The Mössbauer study[17] shows that the substitution of Ni for Fe has a preference to locate at the c sites. In Fe_3NiN at least 80 at. % of Ni atoms locate at the c sites,[10] but until $x=0.5$ all of the c sites are completely occupied by Ni atoms. The atoms at c sites are surrounded by 12 nearest-neighbor atoms at the f site, while the atoms at f sites have two nitrogen atoms as its nearest neighbors. The lattice constant of $(Fe_{1-x}Ni_x)_4N$ decreases with the increase of the Ni content due to the smaller atomic radius of Ni. According to the experimental results,[18] the unit cell volume of $FeNi_3N$ is 1.3% larger than that of Ni_4N (Ref. 22) while 2.9% smaller than that of Fe_4N.

The rest of the paper is organized as follows. We describe briefly the LMTO method and the calculation techniques in Sec. II. In Sec. III the calculated results for the electronic structure of $(Fe_{1-x}Ni_x)_4N$ are presented and the dependence of electronic structure parameters on Ni content is discussed. According to the calculated results, the local magnetic properties of $(Fe_{1-x}Ni_x)_4N$ are discussed in detail in Sec. IV. Finally in Sec. V the volume effects of Ni on the local magnetic moment and the Fermi-contact hyperfine field of $(Fe_{1-x}Ni_x)_4N$ are investigated and some numerical results are presented. Some concluding remarks are included in Sec. VI.

II. LMTO METHOD AND CALCULATION TECHNIQUES

Using the LMTO method which is described and reviewed elegantly in Refs. 23,24, we here perform a semirelativistic spin-polarized band calculation on the $(Fe_{1-x}Ni_x)_4N$ compounds which are isostructural with γ'-Fe_4N. For the merits and disadvantages of the method, as

well as the technique details, refer to Refs. 23,24. In our calculation, the exchange-correlation term is taken as the form deduced by von Barth and Hedin.[25] The Brillouin-Zone integration is carried out for 286 $\vec{k}$-points in the irreducible zone. For valence electrons, which are 3*d*, 4*s* electrons for Fe and Ni and 2*p* electrons for N, we use partial waves to up $l=2$ for Fe and Ni, and apply *s*,*p* orbitals for N. The convergence is assumed when the root-mean-square error of the self-consistent potential is smaller than 1 mRy.

In the atomic-sphere approximation (ASA) the atomic radius assigned to the atomic sites should be chosen so as to satisfy $V=(4\pi/3)\Sigma_i Q_i S_i^3$, where V is the volume of unit cell, and S_i is the atomic radius of the equivalent Q_i atoms in the cell. For $(Fe_{1-x}Ni_x)_4N$, we take the same radius for the same metallic atom located at the *c* and *f* sites, and so the values of S_{Fe},S_{Ni}, and S_N must be well chosen. In addition $S_{Fe}/S_{Ni}=1.023$,[26] $S_N/S_{Fe}=0.68$ are chosen. So the values of S_{Fe},S_{Ni}, and S_N are automatically defined by the above equation in accordance with the cell volume.

The calculations are performed for $(Fe_{1-x}Ni_x)_4N$, where $x=0$, 0.25, 0.5, 0.75, 1.0. The corresponding lattice constants are taken from previous work.[17,19,22]. From Fe_4N to Ni_4N, the unit cell volume decreases about 4.1%. In order to simplify the calculation, for $x=0.25$, we have also applied the model given by Mohn *et al.*[15] and considered that the Ni atoms all locate at the *c* site, although that is not true. For $x=0.5$ and 0.75, there are 1 and 2 Ni atoms located disorderly at the *f* sites in an unit cell except the Ni atom at the *c* site, respectively. To reduce the ordered effect in our calculations, we have calculated all occupation probabilities of Ni^f for the two compositions ($x=0.5$,0.75) and taken their averaged-weight value as final results.

The Fermi-contact hyperfine field H_{FC} and the isomer shift (IS) at each site are calculated according to the prescription given by Akai *et al.*[27] Moreover, here we would like to point out that, since the calculated results are sensitive to the chosen atomic radius and affected by the choice of the exchange-correlation potentials, it is inevitable that there will be some quantitative errors when we compare the calculated results with the experimental results. But nevertheless the qualitative agreement with the experimental results is meaningful.

III. DENSITY OF STATES AND ELECTRONIC STRUCTURE OF $(Fe_{1-x}Ni_x)_4N$

Some electronic structure parameters calculated on $(Fe_{1-x}Ni_x)_4N$ are listed in Table I, in which E_F denotes the Fermi level of system, n_d is the occupation number of spin-polarized *d* electrons (spin down or spin up), C_d defines the center of the *d* partial bands relative to E_F, and γ is the coefficient of electronic specific heat. Using the calculated valence charge density at nucleus $\rho_s(0)$ and the calibration constant $\alpha=-0.24a_0^3$ mm sec^{-1},[27] we have calculated the IS relative to that of α-Fe at Fe and Ni in $(Fe_{1-x}Ni_x)_4N$ and also present the results in Table I. Although the calculated IS at Ni is beyond its actual meaning, the changes of them with the Ni content reveal the changes of $\rho_s(0)$ at these sites.

Although in unit cell the average valence electron number of metal is raised from 8 for $x=0.0$ to 10 for $x=1.0$ due to the more conduction electrons of Ni atom, one can see from the table, a decrease of the calculated E_F occurs with the substitution of Ni for Fe in $(Fe_{1-x}Ni_x)_4N$. The decrease of E_F comes from the decrease of the electron energy in the bands and has generally implied an energy shift of band weight towards lower energy or a narrowed band. The reason produced the decrease can be clarified from the following discussion about the center C_d of *d* partial bands and the occupation number n_d of the electron in the *d* subband. The C_d in Table I show that, with the increase of the *x*, the center of *d* partial band with spin up and spin down of Fe^f move towards lower energy, while those of Ni (Ni^c and Ni^f) move closer to E_F. It can be further seen from the density of states (DOS) (shown in Fig. 1) that $(Fe_{1-x}Ni_x)_4N$ exhibits weak itinerant ferromagnetism. The shifts of *d* partial bands towards higher or lower energy will decrease or increase n_d for both spin directions. In accordance with the changes of the C_d, the n_d at Fe should be raised with the increase of *x*, and that at Ni should be decreased. But the listed n_d at Fe and Ni in Table I indicate that, with the increase of *x*, n_d at Fe^f with spin up increases and that at Fe^f with spin down decreases, while the change of n_d at Ni (Ni^c and Ni^f) is opposite. With the consideration of the changes in the calculated n_d at Fe and Ni with the increase of *x*, it can be suggested that the whole shift of the spin-up *d* partial band has resulted in the changes of the corresponding C_d with the increase of *x*, while the changes of the spin down *d* partial band width, i.e., the spin-down *d* partial bands of Fe^f, are broadened and those of Ni are narrowed, lead to the changes of the C_d for the spin-down *d* partial band. It indicates also that the decrease of E_F is dominated by the energy shift of the 3*d* subband weight of Fe^f towards lower energy and the narrowed spin down 3*d* subband of Ni.

The spin-projected density of states at each site for $(Fe_{1-x}Ni_x)_4N$ has already been shown in Fig. 1. It can be seen from the figure, the spin-up orbitals of Fe(Ni) at each site for all cases of *x* are almost completely occupied. The shape of the DOS, on the whole, changes little with the increase of *x* except for a slight shift. On the contrary, the pronounced peak for their spin-down bands (especially for that of Fe^f) corresponds to vacant states and vary drastically. It is the changes that result in the variation of the local magnetic properties of $(Fe_{1-x}Ni_x)_4N$ (see the following section). The DOS, $N(E_F)$, at E_F is mainly contributed by the spin-down states of metallic atoms and increases from $x=0.25$ to $x=1.0$. Compared with $N(E_F)$ for $x=0$, the smaller exchange splitting at Ni^c than at Fe^c leads to a small reduction of $N(E_F)$ for $x=0.25$. Using the expression $\gamma=\frac{1}{3}\pi^2 k_B^2 N(E_F)$ for the coefficient of electronic specific heat γ, we have calculated γ and listed the results in Table I. Here we must point out that the value of γ for $x=0$ is smaller than our published result[28] due to the use of different calculation parameters. Because of a similar reason the γ for $x=0.25$ is smaller than that deduced from the corresponding $N(E_F)$ by Mohn.[15]

It can be found from Fig. 1 that the interaction between Ni^f and N is very similar to that between Fe^f and N. Except for large interaction states which form a narrow band between Fe^f(Ni^f) *s* and the N *s* near from -0.9 to -0.8 Ry and shows little interaction with other states, there is strong

TABLE I. Some calculated electronic structure parameters on $(Fe_{1-x}Ni_x)_4N$. n_d in electrons/spin, C_d relative to E_F and in Ry, E_F in Ry, γ in mJ/mol K^2, and IS in mm/sec.

		Fe^c		Fe^f		Ni^c		Ni^f	
x		↑	↓	↑	↓	↑	↓	↑	↓
	n_d	4.82	1.64	4.35	2.28				
	C_d	−0.167	−0.089	−0.167	−0.140				
0	E_F			−0.158					
	γ			11.78					
	IS	0.05		0.31					
	n_d			4.39	2.18	4.83	3.77		
	C_d			−0.181	−0.149	−0.140	−0.100		
0.25	E_F			−0.167					
	γ			10.83					
	IS			0.33		−0.22			
	n_d			4.44	2.11	4.82	3.77	4.60	4.05
	C_d			−0.193	−0.160	−0.144	−0.101	−0.171	−0.152
0.5	E_F			−0.171					
	γ			13.55					
	IS			0.32		−0.17		0.10	
	n_d			4.46	2.06	4.80	3.80	4.51	4.15
	C_d			−0.201	−0.163	−0.134	−0.089	−0.162	−0.147
0.75	E_F			−0.191					
	γ			15.84					
	IS			0.35		−0.08		0.15	
	n_d					4.76	3.89	4.43	4.29
	C_d					−0.110	−0.068	−0.154	−0.147
1.0	E_F			−0.226					
	γ			18.06					
	IS					0.06		0.24	

and extensive interaction between $Fe^f(Ni^f)$ and N. $Fe^f(Ni^f)$ d and N p form strong σ and σ^* bonds near -0.5 to 0.25 Ry and a weak π and π^* bond near -0.5 to 0.0 Ry. These agree with those reported by Mohn.[15] The antibonding π^* lies above the main d DOS and near E_F for the spin-up case. This π^* DOS near E_F is responsible for making the systems weak itinerant ferromagnets. With the increase of the Ni content, the π^* antibonding states for both directions of spin move closer to each other and then the corresponding exchange splitting is reduced. Compared with the interaction between $Fe^f(Ni^f)$ and N, those atoms at c site interact little with N since they are too far apart, but much interaction with their nearest-neighbor Fe^f or Ni^f is exhibited. The interaction can be well explained within the model of covalent magnetism.[29]

The calculated IS at Fe and Ni in $(Fe_{1-x}Ni_x)_4N$ indicates a smaller $\rho_s(0)$ at the f site than that at c site. This is similar to that in Fe_4N (Ref. 5) and comes from the stronger interaction between N p and Fe^f (Ni^f) d. On the other hand, it can be found that the $\rho_s(0)$ at Ni (both Ni^c and Ni^f) is much larger than that at Fe. It is probably caused by the larger number of valence electrons but smaller atomic radius of Ni compared to Fe. Generally the reduction of the unit cell volume results in the volume compression of $4s$ conduction electrons and therefore decreases the IS. But it is of interest to find from our calculated results listed in Table I that with the increase of x, the IS at Ni is increased. That means the $\rho_s(0)$ at Ni decreases with the increase of x. It is suggested that the reduction of unit cell volume due to the substitution of Ni leads to a stronger Ni^f-N interaction and results in a stronger shielding effect of the $3d$ electron at Ni^c. At the same time, our calculated IS at Fe^f increases with x, too. When $x \geqslant 0.5$, it does not agree well with the experimental results where the IS at Fe^f is reduced.[30] This disagreement comes perhaps from the excessive Fe-N interaction produced by the large ratio of the Fe and N atomic radius. To understand the change of $\rho_s(0)$ at Fe and Ni, we have fitted the IS at Fe^f and Ni with functions of unit cell volume and obtained the decrease of the $\rho_s(0)$ with the reduction of the unit cell volume by $d\rho_{Fe^f}/d\ln V = 3.4a_0^{-3}$, $d\rho_{Ni^c}/d\ln V = 32.8a_0^{-3}$, and $d\rho_{Ni^f}/d\ln V = 31.9a_0^{-3}$. It is obvious that the $\rho_s(0)$ at Ni decreases more quickly with the reduction of the unit cell volume than at Fe.

IV. LOCAL MAGNETIC PROPERTIES OF $(Fe_{1-x}Ni_x)_4N$

The local magnetic moment μ_{loc} and the Fermi-contact hyperfine field H_{FC} at Fe and Ni calculated on

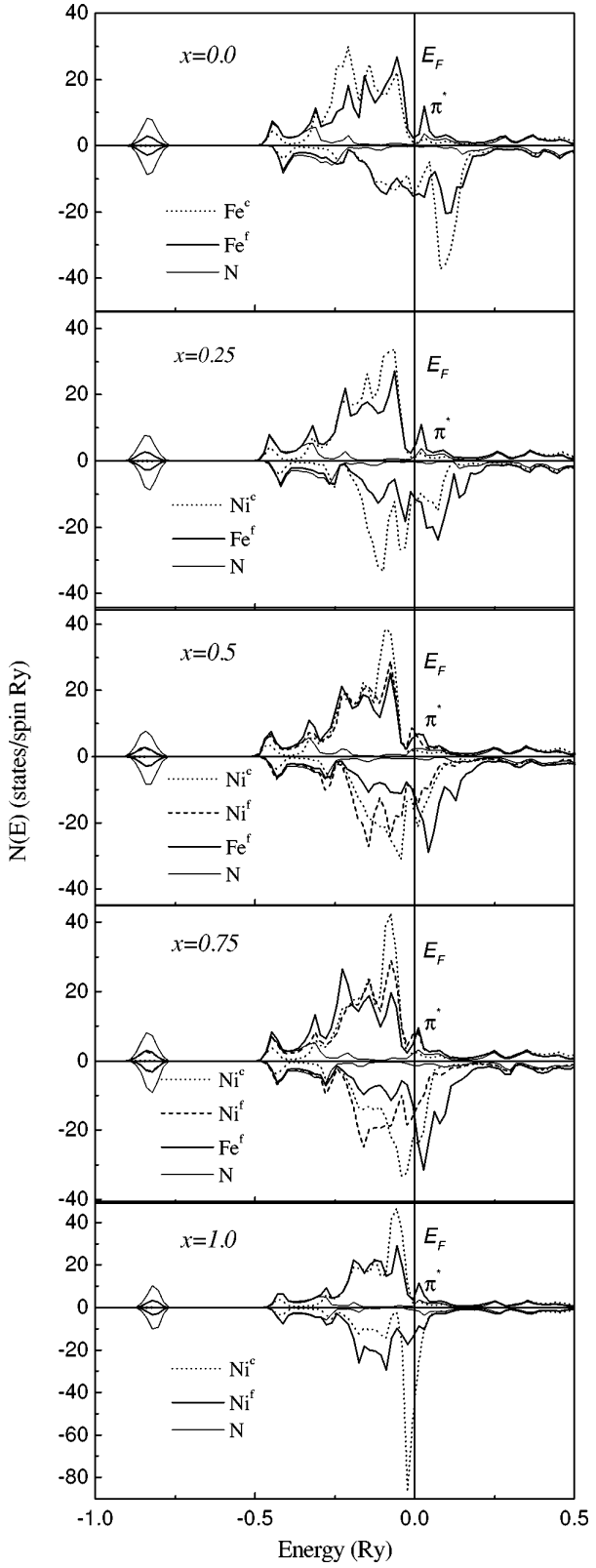

FIG. 1. The calculated spin-polarized local DOS at each site in $(Fe_{1-x}Ni_x)_4N$.

$(Fe_{1-x}Ni_x)_4N$ and their average value $\overline{\mu}$ and $\overline{H_{FC}}$ are listed in Table II. For convenient comparison with the experiments, here the $\overline{H_{FC}}$ is only averaged on the Fe site. Some experimental results are also given in the table.

A. Local magnetic moment of $(Fe_{1-x}Ni_x)_4N$

Due to the substitution of Ni for Fe the $\overline{\mu}$ on Fe and Ni in unit cell is drastically reduced from $2.29\mu_B$ for Fe_4N to $0.32\mu_B$ for Ni_4N. Assuming a proportional relation between the $\overline{\mu}$ and Ni content, we have obtained the reduction of $\overline{\mu}$ by $d\overline{\mu}/dx=-1.91\mu_B$ that agrees well with the slope of the Slater-Pauling curve $d\overline{\mu}/dx=-\delta Z\mu_B$ for Ni alloys containing Fe or Co, where δZ is the difference between the two metal valences. It can be found from the table that the calculated $\overline{\mu}$ for $(Fe_{1-x}Ni_x)_4N$ also agrees well with the results of the magnetization measurement at 1.5 K.[30]

Considering the μ_{loc} at an individual site, we can find that the changes of μ_{loc} depend upon both the atom and the site. In contrast to the small variation of μ_{loc} at Ni^c, with the increase of x, μ_{loc} at Fe^f and Ni^f changes drastically with a different tendency. The μ_{loc} at Fe^f increases with x while that at Ni^f decreases quickly. In $(Fe_{1-x}Ni_x)_4N$ the μ_{loc} at Fe and Ni can be decomposed into two parts from the d electrons and the s,p electrons. In combination with n_d listed in Table I, it is suggested that the changes of the μ_{loc} at Ni^f and Fe^f come mainly from the d electrons. The reduction of the spin-down n_d at Fe^f and the simultaneous increase of spin-up n_d with the increase of x has caused the larger exchange splitting at the site, while the smaller exchange splitting at Ni^f with the increase of x has been produced by the larger n_d at the site. On the contrary, the changes of the sp moment contributes largely to the variation of the μ_{loc} at Ni^c. The sp moment increases from $-0.12\mu_B$ for $x=0.25$ to $0.01\mu_B$ for $x=1.0$ and makes the μ_{loc} at Ni^c not linearly decreasing with the increase of x. It is suggested that the sp polarization at Ni^c caused by Ni^f is positive and by Fe^f negative. This agrees with the result by Mohn.[15]

In Fig. 2(a) we show the dependences of μ_{loc} at Fe^f and Ni on the volume of the unit cell. In spite of the nonlinear dependence of μ_{loc} on the unit cell volume, using the formula $\ln\mu_{loc}=A+B\ln V$, we can fit the volume dependence of the μ_{loc} at Fe^f and Ni^f. The fitting results indicate that the μ_{Fef} increases with the reduction of the unit cell volume by $d\ln\mu_{Fef}/d\ln V=-5.5$ and the μ_{Nif} decrease by $d\ln\mu_{Nif}/d\ln V=75.1$.

B. Hyperfine field of $(Fe_{1-x}Ni_x)_4N$

Concerning the μ_{loc} and the electronic structure of the atom, the calculated H_{FC} at Fe and Ni in $(Fe_{1-x}Ni_x)_4N$ listed in Table II depends also upon the Ni content. The H_{FC} is the main source of hyperfine field H_{hf} in $3d$ transition metal compounds with cubic symmetry. It is closely related to the magnetism of the material and can be decomposed into the core contribution H_{FC}^{core} and the valence contribution H_{FC}^{val}. Compared with the former, the latter is generally a smaller contribution to H_{FC}. In comparison to the experimental results, the values of calculated average Fermi-contact hyperfine field $\overline{H_{FC}}$ on Fe agree well with the average Fe hyperfine field $\overline{H_{hf}}$ (Ref. 30) at 77 K by the Mössbauer effect (ME).

The calculated results indicate the $|\overline{H_{FC}}|$ decreases rapidly with the increase of x. The reduction of the $|\overline{H_{FC}}|$ is different than the change of the average Fe magnetic moment with x and mainly caused by the changes of the interaction between

TABLE II. Calculated local magnetic moments $\mu_{\rm loc}$ (in μ_B) and Fermi-contact hyperfine field $H_{\rm FC}$ (in T) on $(Fe_{1-x}Ni_x)_4N$. Some experimental results (taken from Refs. 1 and 30) are also listed in the table.

	x	Fe^c		Fe^f		Ni^c		Ni^f		average	
		cal.	exp.	cal.	exp.	cal.	exp.	cal.	exp.	cal.	exp.
$\mu_{\rm loc}$	0.0	3.13	2.98	2.01	2.01					2.29	2.21
	0.25			2.17		0.94				1.86	1.69
	0.5			2.33		0.98		0.50		1.55	1.40
	0.75			2.42		0.97		0.34		1.02	
	1.0					0.88		0.13		0.42	
$H_{\rm FC}$	0.0	−42.4	36.2	−35.0	23.1					−36.8	26.4
	0.25		39.0	−27.9	22.0	−38.8				−27.9	24.2
	0.5			−21.0	21.7	−32.7		−13.3		−21.0	21.7
	0.75			−18.6		−20.0		−6.1		−18.6	
	1.0					−6.4		−3.8			

Fe and their neighbors. The reduction of the $|\overline{H_{\rm FC}|}$ with the increase of x can be numerically obtained by $d|\overline{H_{\rm FC}|}/dx = -24.6$ T. It is also noticed that the values of $H_{\rm FC}$ at Fe^f and Ni all decrease rapidly with the increase of the Ni content. The calculated $H_{\rm FC}$ at Fe^f agrees qualitatively well with the $H_{\rm hf}$ at 77 K by ME, too. The volume dependences of the $H_{\rm FC}$ at Fe^f and Ni have also been illustrated in Fig. 2(a), in which we can clearly observe the effects of the substitution of Ni on the $H_{\rm FC}$. Assuming a linear relation between $\ln|H_{\rm FC}|$ and $\ln V$, we can obtain the changes of the $H_{\rm FC}$ by

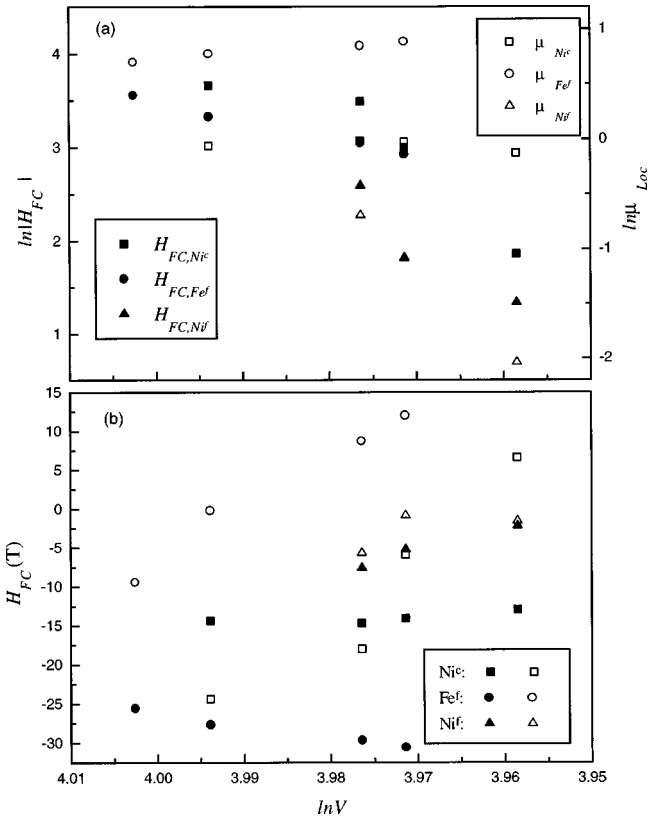

FIG. 2. The unit cell volume dependence of the $H_{\rm FC}$ and the $\mu_{\rm loc}$ at Fe and Ni in $(Fe_{1-x}Ni_x)_4N$. In (b) the filled symbols represent the $H_{\rm FC}^{\rm core}$ and the hollowed symbols indicate the $H_{\rm FC}^{\rm val}$.

$d\ln|H_{{\rm FC},Fe^f}|/d\ln V = 19.3$, $d\ln|H_{{\rm FC},Ni^c}|/d\ln V = 49.7$, and $d\ln|H_{{\rm FC},Ni^f}|/d\ln V = 63.4$. The changes of the $H_{\rm FC}$ at Fe^f and Ni with the increase of x exhibit different characters when compared to those of the $\mu_{\rm loc}$ at Fe and Ni. The change of the $H_{\rm FC}$ at Fe^f with x is even reversed to those of the $\mu_{\rm loc}$ at the site.

To understand the discrepancy between the changes of the $\mu_{\rm loc}$ and the $H_{\rm FC}$ at Fe and Ni atoms, we have decomposed $H_{\rm FC}$ into $H_{\rm FC}^{\rm core}$ and $H_{\rm FC}^{\rm val}$. The former comes from the polarization of the core due to the polarized d electrons and is proportional to the local magnetic moment $\mu_{\rm loc}$ of the atom, while the latter is mainly contributed by the transferred hyperfine field $H_{\rm FC}^{t,{\rm val}}$, which is induced by the sd hybridization between the s orbitals of the atom and the spin-polarized d orbitals of the neighboring atoms, and is proportional to the average magnetic moment μ_{NN} of neighbors, i.e.,[27,31]

$$H_{\rm FC} = H_{\rm FC}^{\rm core} + H_{\rm FC}^{\rm val} = A\mu_{\rm loc} + B\mu_{NN},$$

where A and B are defined as hyperfine coupling constants.

The unit cell volume dependences of $H_{\rm FC}^{\rm core}$ and $H_{\rm FC}^{\rm val}$ at Fe^f and Ni are given in Fig. 2(b), in which the filled symbols represent the $H_{\rm FC}^{\rm core}$ while the hollow symbols represent the $H_{\rm FC}^{\rm val}$. It is shown that the $H_{\rm FC}^{\rm core}$ is the main contribution to $H_{\rm FC}$ for Fe^f while $H_{\rm FC}^{\rm val}$ plays an important role for Ni^c and Ni^f. But commonly, the volume dependences of the $H_{\rm FC}^{\rm core}$ values at all the sites are similar to those of the corresponding $\mu_{\rm loc}$ shown in Fig. 2(a)—in contrast with the case $H_{\rm FC}^{\rm val}$ at these sites. So the $\mu_{\rm loc}$ dependence of the $H_{\rm FC}^{\rm core}$ at Fe and Ni sites in $(Fe_{1-x}Ni_x)_4$ N can be extracted. The proportionality coupling constant A changes little with the increase of the x and is evaluated to be about -12.7 T/μ_B for Fe^f which is comparable with the result of Fe_4N,[8] -14.9T/μ_B and -15.8T/μ_B for Ni^c and Ni^f, respectively.

The change of $H_{\rm FC}^{\rm val}$ (approximately $H_{\rm FC}^{t,{\rm val}}$) at Fe^f and Ni sites with the unit cell volume is quite different from that of the $H_{\rm FC}^{\rm core}$. The $H_{\rm FC}^{\rm val}$ at Fe^f and Ni^c increase with the reduction of unit cell volume and even change from a negative to a positive contribution to $H_{\rm FC}$, but that at Ni^f retains a negative contribution and there is a maximal $H_{\rm FC}^{\rm val}$ when $x = 0.75$. With the consideration of the neighboring interaction be-

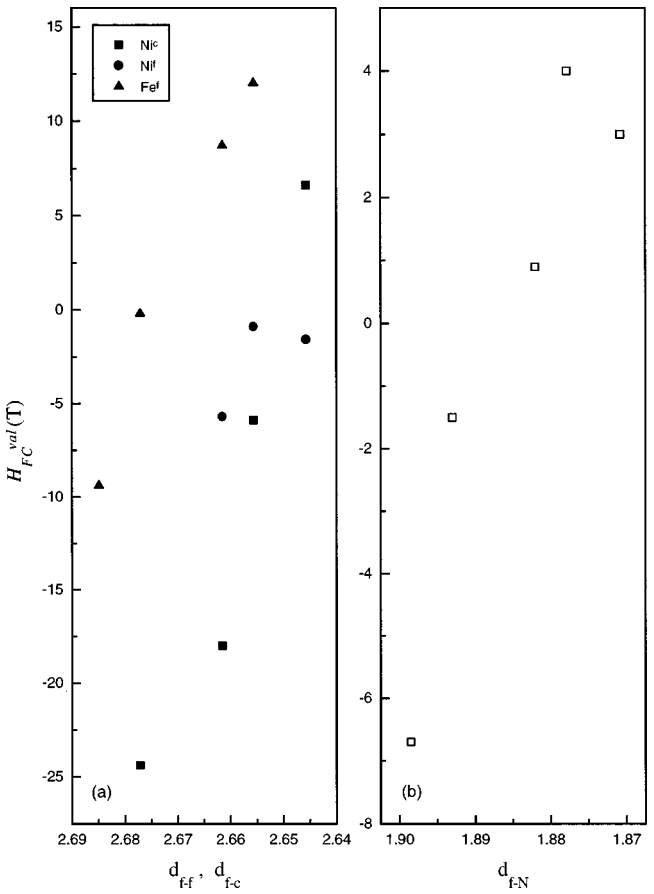

FIG. 3. The dependence of the $H_{\mathrm{FC}}^{\mathrm{val}}$ at metallic atoms (a) and N (b) in $(\mathrm{Fe}_{1-x}\mathrm{Ni}_x)_4\mathrm{N}$ on the interatomic distance with nearest neighbors.

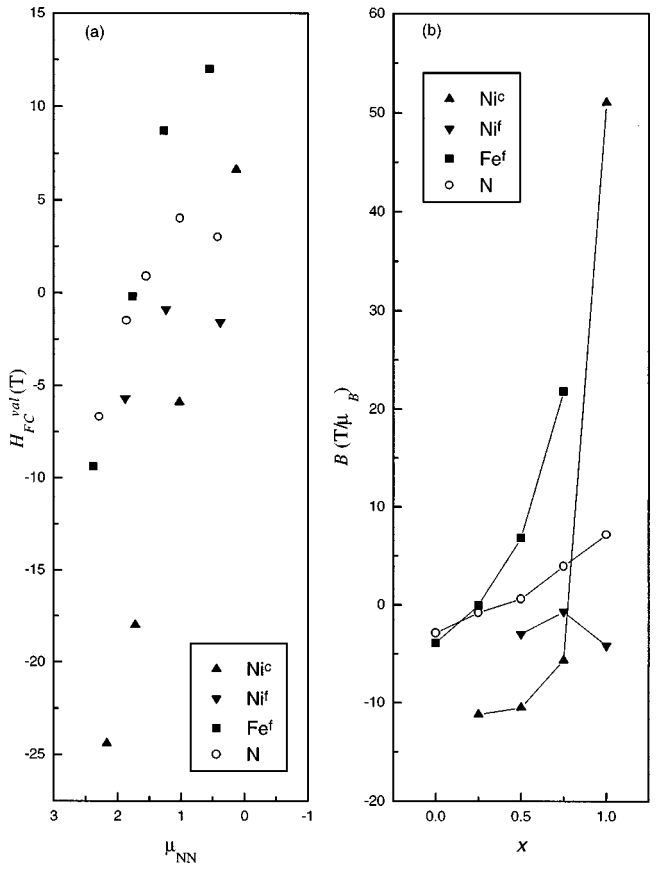

FIG. 4. The $H_{\mathrm{FC}}^{\mathrm{val}}$ (a) and the hyperfine coupling constant B (b) at each site in $(\mathrm{Fe}_{1-x}\mathrm{Ni}_x)_4\mathrm{N}$ as functions of the μ_{NN} and the x, respectively.

tween metallic atoms in $(\mathrm{Fe}_{1-x}\mathrm{Ni}_x)_4\mathrm{N}$, the $H_{\mathrm{FC}}^{\mathrm{val}}$ at the c site comes from the sd hybridization of the s orbitals with the spin-polarized d orbitals of atoms at the f sites, while the $H_{\mathrm{FC}}^{\mathrm{val}}$ at the f sites is produced not only by the sd hybridization with the atoms at the c site but also by the sd hybridization with the neighboring atoms at the f sites. We have illustrated the changes of the $H_{\mathrm{FC}}^{\mathrm{val}}$ at Fe^f and Ni with the interatomic distance with a neighboring metallic atom in Fig. 3(a) to understand the effect of the change of interatomic interaction on $H_{\mathrm{FC}}^{\mathrm{val}}$. With the increase of x, the atomic distances in the unit cell are decreased and the interaction between atoms are strengthened, in turn the interatomic sd hybridization is also enlarged. So the $H_{\mathrm{FC}}^{\mathrm{val}}$ at Fe^f and Ni^c increase greatly. The maximum of $H_{\mathrm{FC}}^{\mathrm{val}}$ at Ni^f when $x=0.75$ indicates that the variation of the interaction caused by the substitution of Ni and the reduction of atom distance. As mentioned above, $H_{\mathrm{FC}}^{\mathrm{val}}$ is proportional to μ_{NN} and reveals the influence of the neighbors on H_{FC} via the hyperfine coupling constant B between atoms. The $H_{\mathrm{FC}}^{\mathrm{val}}$ at Fe^f and Ni in $(\mathrm{Fe}_{1-x}\mathrm{Ni}_x)_4\mathrm{N}$ are shown in Fig. 4(a) as functions of μ_{NN}. Among them, the sign reverse and the nonlinear variation of the $H_{\mathrm{FC}}^{\mathrm{val}}$ at Fe^f and Ni with μ_{NN} indicate the change of coefficient B with the increase of x [shown in Fig. 4(b)] and reveals also the variation of the interaction between the atom and its neighbors. The larger B value at Ni^c implies the stronger interaction between Ni^c and its neighbors when compared to interaction between Fe^f and its neighbors.

It is also of interest to study the H_{FC} at N in $(\mathrm{Fe}_{1-x}\mathrm{Ni}_x)_4\mathrm{N}$. It can be decomposed as a metallic atom. From the results listed in Table III, it can be seen that the main source of the H_{FC} is $H_{\mathrm{FC}}^{\mathrm{val}}$, in which the transferred hyperfine field from the neighboring $\mathrm{Fe}^f(\mathrm{Ni}^f)$ dominates. In Fig. 3(b) and Fig. 4(a) we have illustrated the change of $H_{\mathrm{FC}}^{\mathrm{val}}$ at N with atomic distance d_{f-N} with neighbors and with the μ_{NN}, respectively. The change of $H_{\mathrm{FC}}^{\mathrm{val}}$ at N with d_{f-N} and μ_{NN} is similar to that of Ni^f but the $H_{\mathrm{FC}}^{\mathrm{val}}$ of N change from a negative to a positive contribution when $x \geqslant 0.5$. The change of $H_{\mathrm{FC}}^{\mathrm{val}}$ at N reveals that the $\mathrm{Fe}^f(\mathrm{Ni}^f)$-N interaction varies strongly with the decrease of the unit cell volume and the average magnetic moment. Generally speaking, a positive contribution to the $H_{\mathrm{FC}}^{\mathrm{val}}$ of N is induced by antibonding states and a negative one by bonding states. Our results indicate that the bonding states are favored in the cases of low x, while the antibonding states dominate the $H_{\mathrm{FC}}^{\mathrm{val}}$ of N for the cases of higher Ni content.

TABLE III. Calculated Ferm-contact hyperfine field H_{FC} and $H_{\mathrm{FC}}^{\mathrm{val}}$ (in T) of N in $(\mathrm{Fe}_{1-x}\mathrm{Ni}_x)_4\mathrm{N}$.

x	0.0	0.25	0.50	0.75	1.0
H_{FC}	−7.0	−1.1	1.3	4.8	3.2
$H_{\mathrm{FC}}^{\mathrm{val}}$	−6.7	−1.5	0.9	4.0	3.0

V. VOLUME EFFECT OF THE Ni ATOM IN $(Fe_{1-x}Ni_x)_4N$

Summarizing the above discussion, one can find the substituted Ni atom plays an important role in determining the properties of $(Fe_{1-x}Ni_x)_4N$. The substitution of Ni for Fe has caused a smaller unit cell volume of $(Fe_{1-x}Ni_x)_4N$ due to its smaller radius and resulted in the variation of interaction between atoms in the unit cell due to the different properties of Ni compared to Fe. So, the effects of the substituted Ni atom may be divided into two parts: one is the volume effect produced by the reduction of unit cell volume and the other is the chemical bonding effect caused only by the change of the interaction between atoms. The combination of the two effects dominates the change of the properties of $(Fe_{1-x}Ni_x)_4N$ with x. In light of this consideration, the change of quantity A with the Ni content or unit cell volume can be written as

$$\frac{dA}{dx}=\left(\frac{\partial A}{\partial x}\right)_V+\left(\frac{\partial A}{\partial \ln V}\right)_x\cdot\frac{\partial \ln V}{\partial x}$$

or

$$\frac{dA}{d\ln V}=\left(\frac{\partial A}{\partial \ln V}\right)_x+\left(\frac{\partial A}{\partial x}\right)_V\cdot\frac{\partial x}{\partial \ln V},$$

where $(\partial A/\partial \ln V)_x$ is the volume effect of Ni atom and $(\partial A/\partial x)_V$ is the chemical bonding effect. For $(Fe_{1-x}Ni_x)_4N$, $\partial \ln V/\partial x=-4.43\times10^{-2}$.

To distinguish the volume effect of Ni from the chemical bonding effect, we have calculated the electronic structure of volume-expanded $(Fe_{1-x}Ni_x)_4N$, which retains the lattice constants of Fe_4N and whose volume does not decrease with the increase of x. Then the variation of the calculated results with x is caused only by the pure chemical bonding effect of Ni. The difference of the results from those of normal $(Fe_{1-x}Ni_x)_4N$ represents the volume effect of Ni.

The calculated $\overline{\mu}$ for volume-expanded $(Fe_{1-x}Ni_x)_4N$ decreases with the increase of x by $(\partial\overline{\mu}/\partial x)_V=-1.90\mu_B$. Comparing that with the result in normal $(Fe_{1-x}Ni_x)_4N$, we obtain $(\partial\overline{\mu}/\partial \ln V)_x=0.22\mu_B$, which is the volume effect of Ni on $\overline{\mu}$. Similarly, the effect of Ni on the $\mu_{\rm loc}$ at Fe^f can be divided into a chemical bonding effect with $(\partial \ln\mu_{Fe^f}/\partial x)_V=0.33$ and a volume effect with $(\partial \ln\mu_{Fe^f}/\partial \ln V)_x=1.9$. Here the chemical bonding effect of Ni increases μ_{Fe^f} which is similar to the effect of N in γ'-Fe_4N, while its volume effect decreases μ_{Fe^f}.

In comparison to that on magnetic moment, the effect of Ni on $H_{\rm FC}$ at Fe^f has exhibited different characters. With the increase of x, the value of $H_{\rm FC}$ at Fe^f is reduced by the chemical bonding effect of Ni with $(\partial \ln|H_{{\rm FC},Fe^f}|/\partial x)_V=-0.93$ while raised by the volume effect of Ni with $(\partial \ln|H_{{\rm FC},Fe^f}|/\partial \ln V)_x=-1.7$. This discrepancy, with the effect of Ni on μ_{Fe^f}, is probably caused by the transferred $H_{\rm FC}$ of the neighbors.

Because the result from the volume-expanded $(Fe_{1-x}Ni_x)_4N$ represents the chemical bonding effect of Ni, the investigation on $H_{\rm FC}^{\rm val}$ is very helpful to understand the change of interatomic interaction. The calculated $H_{\rm FC}^{\rm val}$ at each site is shown in Fig. 5(a) as functions of x. The results indicate that, with the increase of x, the less that the Fe atom occupies the f site, the larger the $H_{\rm FC}^{\rm val}$ at Ni^c. The larger that the neighboring Ni atom of Fe^f is, the larger the $H_{\rm FC}^{\rm val}$ at Fe^f. With an assumption that the spin-polarized d orbitals of Fe^f atom produces a negative transferred $H_{\rm FC}^{\rm val}$ at its neighbors while the spin-polarized d orbitals of Ni^c and Ni^f induces a positive transferred $H_{\rm FC}^{\rm val}$ at its neighbors, the changes of the $H_{\rm FC}^{\rm val}$ of Fe^f and Ni^c with x can be well explained. In fact, this is in accordance with our discussion on $\mu_{\rm loc}$. From Fig. 5(a) we can extract the chemical bonding effect of Ni on $H_{\rm FC}^{\rm val}$ at Fe^f with $(\partial H_{{\rm FC},Fe^f}^{\rm val}/\partial x)_V=32.8$ T. For normal $(Fe_{1-x}Ni_x)_4N$ we can obtain $dH_{{\rm FC},Fe^f}^{\rm val}/dx=29.2$ T, then the volume effect of Ni on $H_{\rm FC}^{\rm val}$ at Fe^f is equal to $(\partial H_{{\rm FC},Fe^f}^{\rm val}/\partial \ln V)_x=81.3$ T. This effect decreases the $H_{\rm FC}^{\rm val}$ at Fe^f with the increase of x. When $H_{\rm FC}$ at Fe^f is negative, the volume effect of Ni raises the value of $H_{\rm FC}$ at Fe^f. To understand the volume effect of Ni on the interaction between atoms, we have further plotted the difference of $H_{\rm FC}^{\rm val}$ at Fe^f and Ni in normal $(Fe_{1-x}Ni_x)_4N$ from that in volume-expanded $(Fe_{1-x}Ni_x)_4N$ in Fig. 5(b). It can be seen that, in contrast to the volume effect on Fe^f, the volume effect of Ni makes the $H_{\rm FC}^{\rm val}$ at Ni^f increasing with the reduction of the unit cell volume. The change of $H_{\rm FC}^{\rm val}$ at Ni^c in the cell volume is much complicated, a maximal $H_{\rm FC}^{\rm val}$ occurs when $x=0.5$ and even a reverse of sign when $x=1.0$. The abnormal changes of the $H_{\rm FC}^{\rm val}$ in the unit cell volume have obviously indicated the obvious interatomic distance dependence of the conduction-electron spin-polarization contributing to $H_{\rm FC}^{\rm val}$.

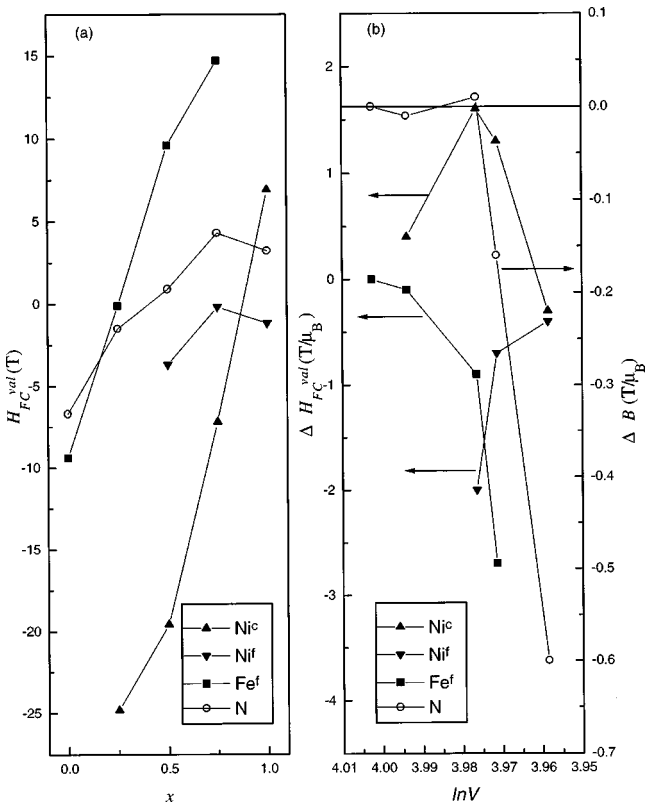

FIG. 5. (a) The calculated $H_{\rm FC}^{\rm val}$ at each sites in volume-expanded $(Fe_{1-x}Ni_x)_4N$. (b) The volume effect of Ni on the $H_{\rm FC}^{\rm val}$ at Fe^f and Ni and the hyperfine coupling constant B at N.

It is worthwhile observing the change of the hyperfine coupling constant B at N due to the volume effect of Ni. In Fig. 5(b) we have also shown the difference of B in normal $(Fe_{1-x}Ni_x)_4N$ from that in volume-expanded $(Fe_{1-x}Ni_x)_4N$. With the reduction of unit cell volume (interatomic distance with the neighbors) the B at N exhibits an oscillating strengthened variation. This indicates that the valence electrons polarization at N due to metallic atoms at f site depends strongly upon the interatomic distance and is very similar to the picture of the RKKY interaction in rare earths.

VI. CONCLUDING REMARKS

We have successfully applied the spin-polarized linear muffin-tin orbital (LMTO) method to calculate the electronic structure of $(Fe_{1-x}Ni_x)_4N$. To our knowledge, it is the first to present the detailed theoretical calculated results on these systems with $x>0.25$. According to our calculated results, the local electronic and magnetic properties of $(Fe_{1-x}Ni_x)_4N$ have been explored and the calculated results agree qualitatively with the experimental results.

(1) The substitution of Ni for Fe affects the electronic structure of $(Fe_{1-x}Ni_x)_4N$. The whole shift of the $3d$ subband weight and the changes of the $3d$ subband width in the cell with the increase of x have induced the decrease of E_F.

(2) The substitution of Ni for Fe leads to a stronger Ni^f-N interaction and results in a stronger shielding effect of the $3d$ electron at Ni^c and then the $\rho_s(0)$ decreases largely with the increase of Ni content in spite of the volume compression of $4s$ conduction electrons.

(3) The discrepancy between the changes of the $\mu_{\rm loc}$ and the $H_{\rm FC}$ with the Ni content indicate the important effect of the transferred $H_{\rm FC}$.

(4) The volume effects of the substituted Ni on the local magnetic moment and the Fermi-contact hyperfine field have been distinguished from the chemical bonding effects. With the increase of the x, the chemical bonding effect of Ni increases $\mu_{{\rm Fe}f}$ but reduces the value of $H_{\rm FC}$ at Fe^f. On the contrary, the volume effect of Ni decreases $\mu_{{\rm Fe}f}$ but raises the value of $H_{\rm FC}$ at Fe^f.

(5) It is of interest to have observed the strong interatomic distance dependence of conduction-electron polarization in cell and even an exhibition of a RKKY-like oscillating variation at N.

ACKNOWLEDGMENTS

The calculations were carried on a DEC-3000 workstation. This project was supported by the NSFC and by the National Education Committee of China.

*Present address: Fakultät für Physik und Astronomie, Institut für Experimentalphysik III, AG Festkörperspektroskopie, Universitätsstr. 150, D-44801 Bochum, Germany. Electronic address: kong@ep3.ruhr-uni-bochum.de

[1] B.C. Frazer, Phys. Rev. **112**, 751 (1958).
[2] J.S. Lord, J.G.M. Armitage, P.C. Riedi, S.F. Matar, and G. Demazeau, J. Phys. Condens. Matter **6**, 1779 (1994).
[3] C.A. Kuhnen, R.S. de Fiqueiredo, V. Drago, and E.Z. da Silva, J. Magn. Magn. Mater. **111**, 95 (1992).
[4] F.S. Li, Y. Kong, and R.J. Zhou, J. Phys. Condens. Matter **7**, L235 (1995); F.S. Li, Y. Kong, R.J. Zhou, C.L. Yang, M.M. Abd-Elmeguid, G. Michels, H. Micklitz, and J.W. Otto, Solid State Commun. **95**, 753 (1995).
[5] C.L. Yang, M.M. Abd-Elmeguid, H. Micklitz, G. Michels, J.W. Otto, Y. Kong, D.S. Xue, and F.S. Li, J. Magn. Magn. Mater. **151**, L19 (1995).
[6] S.F. Mater, P. Mohn, G. Demazeau, and B. Siberchicot, J. Phys. Condens. Matter **49**, 1761 (1988).
[7] Wei Zhou, Lijia Qu, Qiming Zhang, and Dingsheng Wang, Phys. Rev. B **40**, 6393 (1989).
[8] Yong Kong, Rongjie Zhou, and Fashen Li, J. Phys. Condens. Matter **8**, 3829 (1996).
[9] Yong Kong, Rongjie Zhou, and Fashen Li, Phys. Rev. B **54**, 5460 (1996).
[10] G. Shirane, W.J. Takei, and S.L. Ruby, Phys. Rev. B **126**, 49 (1962).
[11] B. Siberchicot, S.F. Matar, L. Fournes, G. Demazeau, and P. Hagenmüller, J. Solid State Chem. **84**, 10 (1990).
[12] D. Andriamandroso, L. Fefilative, G. Demazeau, L. Fournes, and M. Pouchard, Mater. Res. Bull. **19**, 1187 (1984).
[13] S.K. Chen, S. Jin, T.H. Tiefel, Y.F. Hsieh, E.M. Gyorgy, and D.W. Johnson Jr., J. Appl. Phys. **70**, 6247 (1991).
[14] M. Kume, T. Tsujioka, K. Matsuura, and Y. Abe, IEEE Trans. Magn. **MAG-23**, 3633 (1987).
[15] P. Mohn, K. Schwarz, S. Matar, and G. Demazeau, Phys. Rev. B **45**, 4000 (1992).
[16] S.F. Matar, J.G.M. Armitage, P.C. Riedi, G. Demazeau, and P. Hagenmüller, Eur. J. Solid State Inorg. Chem. **26**, 517 (1989).
[17] F.S. Li, J.B. Yang, D.S. Xue, and R.J. Zhou, Appl. Phys. Lett. **66**, 2343 (1995).
[18] J.B. Yang, D.S. Xue, R.J. Zhou, and F.S. Li, Phys. Status Solidi A **153**, 307 (1996).
[19] X.G. Diao, F.S. Li, and S.Q. Zhou, J. Mater. Sci. Lett. **15**, 1590 (1996).
[20] D.L. Williamson and M. Kopcewicz, Hyperfine Interact. **80**, 1043 (1993).
[21] R. Juza, in *Advances in Inorganic Chemistry and Radiochemistry*, edited by H.J. Emcleus and A.G. Sharpe (Academic, New York, 1966), Vol. 9, p. 81.
[22] R. Baranova, Y.O. Khodyrev, and S. Semiletov, Sov. Phys. Crystallogr. **27**, 554 (1982).
[23] O.K. Anderson, Phys. Rev. B **12**, 3050 (1975).
[24] H.L. Skriver, in *The LMTO Method*, edited by M. Cardona, P. Fulde, and H.J. Queisser (Springer, Berlin, 1984).
[25] U. Von Barth and L. Hedin, J. Phys. C **5**, 1629 (1972).
[26] T. Nautiyal and S. Auluck, Phys. Rev. B **47**, 1726 (1993).
[27] H. Akai, M. Akai, S. Blügel, B. Drittler, H. Ebert, Terakura, R. Zeller, and P.H. Dederichs, Prog. Theor. Phys. Suppl. **101**, 11 (1990).
[28] Yong Kong, Rongjie Zhou, and Fashen Li, Phys. Status Solidi B **192**, 87 (1995).
[29] A.R. Williams, R. Zeller, V.L. Moruzzi, C.D. Gelatt Jr., and J. Kübler, J. Appl. Phys. **52**, 2067 (1981).
[30] J.B. Yang, thesis, Lanzhou University, 1995.
[31] Z.M. Stadnik and G. Stronik, Hyperfine Interact. **47**, 275 (1989).